Numerical Analysis of Traveling Waves in Power Systems with Grid Forming Inverters

Frank Miyagishima
Electrical and Computer
Engineering Department
New Mexico State University
Las Cruces, NM 88003
frankjm@nmsu.edu

Olga Lavrova
Electrical and Computer
Engineering Department
New Mexico State University
Las Cruces, NM 88003
olavrova@nmsu.edu

Sijo Augustine
Electrical and Computer
Engineering Department
New Mexico State University
Las Cruces, NM 88003
sijo@nmsu.edu

Satish Ranade
Electrical and Computer
Engineering Department
New Mexico State University
Las Cruces, NM 88003
sranade@nmsu.edu

Matthew J. Reno Sandia National Laboratories Albuquerque, NM, 87185 mjreno@sandia.gov Javier Hernandez-Alvidrez Sandia National Laboratories Albuquerque, NM, 87185 jherna4@sandia.gov

Abstract — This paper presents a simulation and respective analysis of traveling waves from a 5-bus distribution system connected to a grid-forming inverter (GFMI). The goal is to analyze the numerical differences in traveling waves if a GFMI is used in place of a traditional generator. The paper introduces the topic of traveling waves and their use in distribution systems for fault clearing. Then it introduces a Simulink design of said 5-bus system around which this paper is centered. The system is subject to various simulation tests of which the results and design are explained further in the paper to discuss if and how exactly inverters affect traveling waves and how different design choices for the system can impact these waves. Finally, a consideration is made for what these traveling waves represent in a practical environment and how to properly address them using the information derived in this study.

Keywords — Grid forming inverter, inverter based resource, traveling waves, wave reflections, wavelets, Simulink, MATLAB, Fourier transform

I. INTRODUCTION

Electrical power systems are sophisticated networked grids, which need to function with high reliability to provide electricity to customers. With a high number of interconnected buses and devices in both transmission and distribution networks, electrical power systems, grid modernization, and the

This work was partially supported by the NSF Grants \#OIA-1757207 (NM EPSCoR), HRD-1345232, HRD-1914635 and funding from the Laboratory Directed Research and Development program at Sandia National Laboratories, and funding from the Electric Utility Management Program (EUMP) at the New Mexico State University. Sandia National Laboratories is a multi-mission laboratory managed and operated by National Technology and Engineering Solutions of Sandia, LLC., a wholly owned subsidiary of Honeywell International, Inc., for the U.S. Department of Energy's National Nuclear Security Administration under contract DE-NA0003525. The views expressed in the article do not necessarily represent the views of the U.S. Department of Energy or the United States Government.

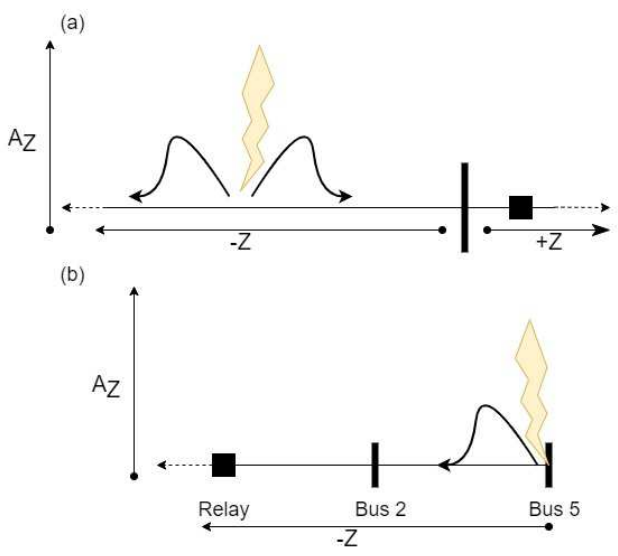


Fig. 1 (a) Example of a traveling wave. Electric current (y-axis) is measured against distance (x-axis). (b) Diagram of wave propagation during a fault on Bus 5.

addition of renewable resources, it is important to continue to develop new methods of detecting and mitigating faults in the system [1, 2].

One such method is the use of what is known as traveling waves to detect the location of faults. When faults occur it is critical to locate the fault, correct the issue that caused it, and bring the system back to regular operation as quickly as possible [3]. This is especially critical because of how fast these systems operate and are prone to randomly occurring failures [4, 5]. Traveling wave protection schemes take advantage of the electric voltage and current "waves" that are reflected across

transmission and distribution lines due to disturbances in the power system. Fig. 1 shows a graphical representation of a traveling wave generated by a fault incident on distribution line. These are then used to calculate the theoretical location of the fault with a relay, so that it may be identified and cleared.

Research into traveling waves goes back as far as the 1950's. Recently in the mid 1990's researchers successfully used wavelet transforms to locate faults [6]. The use of traveling wave based protection in turn also involves using relays with communication and processing units to capture the traveling waves, identify the fault, and handle the protection method for the system.

The goal of this paper is to contribute to the investigation of protection schemes of distribution systems, particularly of DC microgrids which could potentially be a reliable system in commercial use given proper design [7-9]. It should be noted that this paper is based entirely around a practical test simulation model, as explained further in Section II.

II. DESIGN AND PURPOSE OF THE STUDY

A MATLAB/Simulink model of a 5-bus system is developed to understand and analyze the traveling wave protection, a diagram is shown in Fig. 2.

This design is centered around Bus 1, which is connected to a grid-forming inverter (GFMI). The rest of the system entails a single junction relay in between Bus 1 and Bus 2, two loads

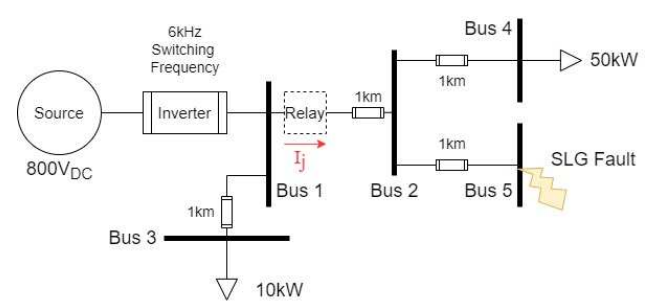


Fig. 2 Topology of system design.

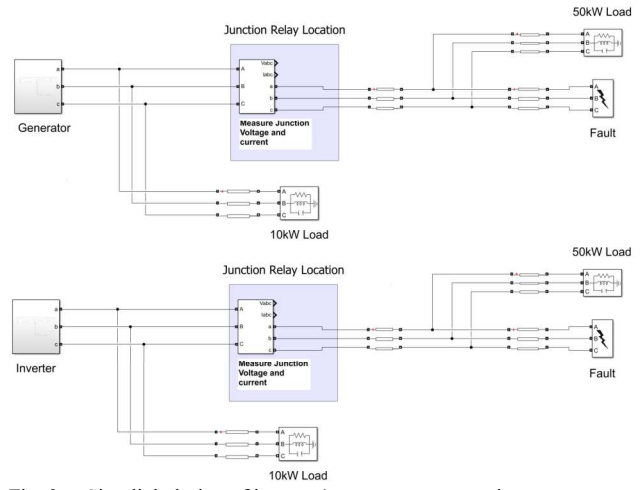


Fig. 3 Simulink design of inverter/generator system pair

and a fault incidence in the other buses. The lengths of the distribution lines between all the buses are 1km. The junction relay is set to measure the A-phase current in its line (denoted by I_a), and such measurements are used to analyze the fault current after the fault incidence as well as the wavelets traveling along the line as a result of the constant switching of the inverter. This is discussed further in Section III.

The purpose of this design is to analyze the impact using a GFM inverter connected to Bus 1 in place of a three-phase generator has on the traveling waves of the system. Further analysis is performed by using different switching frequencies for the inverter. These settings are interchanged on the system and the simulation results of each are compared against each other. Fig. 3 shows an example of this design simulation.

Another important design aspect of note is the filter used in the inverter. In place of the usual LC (inductor-capacitor) filter commonly used in inverters, the GFM inverter employs an LCL (inductor-capacitor-inductor) filter. This is discussed further in Section IV.

III. TRAVELING WAVE REFLECTIONS

It must be declared that connecting Inverter Based Resources (IBRs) has an effect on the traveling waves along the distribution line caused by fault disturbances, as is demonstrated later. However, it is important to quantify the magnitude of these changes. Specifically, what is the difference in traveling wave propagation, reflection, and detection in distribution systems with and without Inverter Based Resources (IBRs) For example, the Pulse Width Modulation (PWM) switching of the inverter, if not carefully filtered at the output stages of the inverter, may create traveling waves of its own as the power system is disturbed slightly each time. Furthermore, GFM inverters may present yet a more sophisticated behavior than regular IBRs due to the fact that they may replace traditional generators in microgrids or during outages [10].

Traveling waves are described as electromagnetic waves which are propagated along the power system equipment (e.g., lines, cables, etc.) as a result of a disturbance in the power system. The disturbances are defined as any fault, lightning, switching, etc [11]. This means that traveling waves generate both due to a fault incident on the system or (to a lesser degree) due to switching, among other reasons.

Fig. 4 shows the current I_a immediately after the fault is applied to Bus 5. Naturally, a traveling "fault wave" originates at the fault location and eventually reaches the relay. This is signified by the sudden "drop" shape of the current shown in the figure. Although this disturbance originated on the grid end of the GFMI, the settings of the inverter still have an effect on the shape, particularly its magnitude. This is seen by comparing the fault wave across three different inverter switching frequencies. The difference is measured between the change in current at the points immediately before and after the drop. At

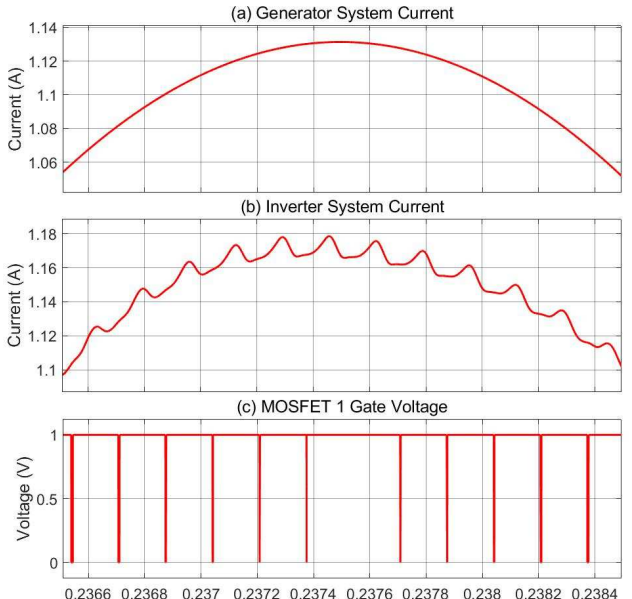


Fig. 5 (a) shows the current I_a in the system connected to the generator, (b) shows I_a in the system connected to the inverter, and (c) shows gate voltage of MOSFET 1 in the inverter (controls a-phase current).

the default 6kHz frequency, the fault wave has a magnitude of 4.3mAp. Lowering the frequency to 4kHz slightly increases the magnitude to 4.5mAp, and increasing the frequency to 10kHz reduces the magnitude down to 1.3mAp. These frequency dependencies require careful analysis of the switching frequency and, by relation, the filter design and what is known "switch waves".

Switching noise-induced traveling waves (switch waves for short) are seen in Fig. 5 where the relay current I_a is compared between a system connected to a generator and a system connected to a GFMI, the figure also shows the gate voltage of the MOSFET controlling I_a in the inverter. As shown in the figure, the switch waves can be seen on the relay in the system with the GFMI but not in the system with a traditional generator, furthermore the MOSFET switching shows a correlation between the switching noise and the switch waves. Fig. 6 further highlights this effect by comparing the Fourier analyses of the current I_a for different switching frequencies. The respective frequency components of each of these graphs reflect the switch wave effect caused by switching noise. It should also be noted that the 10kHz component has a smaller amplitude than the 4kHz component, this is because the filter in

the inverter acts as a lowpass filter which attenuates higher frequencies. This is explained further in Section IV.

IV. FILTER DESIGN

The switch waves require a more complex filter than the usual LC filter employed in most DC/AC inverters, for this purpose an LCL filter is used instead. A transfer function in the form of $H = i_g/v_i$ where i_g is the grid side current and v_i is the output voltage is taken from [12] to measure the approximate attenuation value of the filter used. The transfer function is defined in (1).

$$Hd_{LCL}(s) = \frac{c_f R_f s + 1}{L_1 c_f L_2 s^3 + c_f (L_1 + L_2) R_f s^2 + (L_1 + L_2) s} \tag{1}$$

Where C_f is the capacitance, R_f is the resistance in series with the capacitance, L_1 is the inverter side inductance, and L_2 is the grid side inductance [13-15]. For the purpose of this design L_1 and L_2 have the same value. Given an inductance of $800\mu H$ and a capacitance of $150\mu F$ of the LCL filter, the attenuation at the switching frequency of 6kHz is -20.9dB.

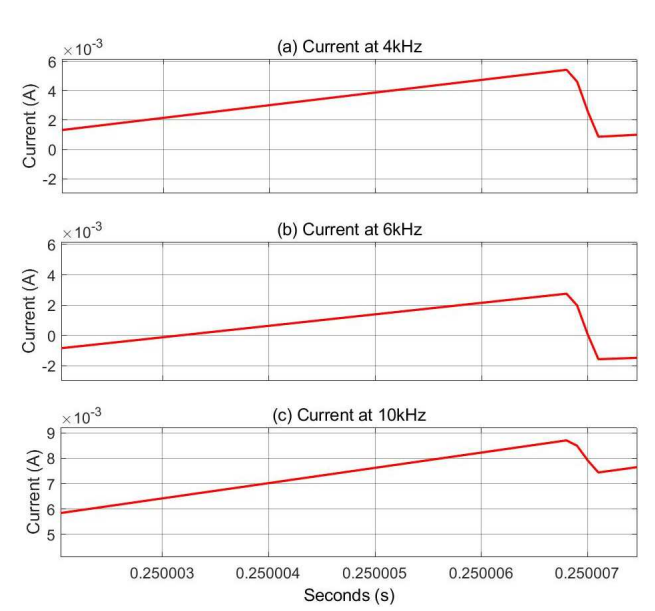


Fig. 4 Current I_a immediately after the fault inception for a system connected to an inverter with (a) 4kHz switching frequency, (b) 6kHz, and (c) 10kHz.

For reference, an additional simulation is executed to compare four different LCL parameters and the effect the attenuation has on the switch waves. A simple method of analyzing the attenuation is comparing the ratios of the magnitude of the wavelet at 100% duty ratio (which occurs at 0.2375s) with the peak magnitude of the current I_a sine wave. This comparison is supplemented with another Fourier transform for each filter design as depicted in Fig. 7, where the filters are listed as F1, F2, F3, and F4 according to the parameters defined in Table 1. In this case, the amplitude of the frequency components for 6kHz (switching frequency) and 60Hz (base frequency) are compared to each other.

TABLE I. LCL FILTER COMPARISON

	1000μH 175μF "F1"	800μH 150μF "F2"	600μH 125μF "F3"	400μH 100μF "F4"
Wavelet/ I_a ratio (%)	0.286	0.544	0.792	1.45
SNR _{dB} (%)	27.58	25.97	23.96	21.25
Attenuation at 6kHz (dB)	-28.2	-20.9	-7.97	-2.56

As shown in Table 1, the filter capacitance and inductance values decrease from F1 to F4. As F1 is the largest filter, it has the highest attenuation for 6kHz and thus the magnitude of that frequency component is noticeably smaller than for the F4 filter. This means larger filters have a better performance than smaller ones. The four peaks shown in each spectrum in Fig. 7 represent the combined frequencies of 6kHz and the base frequency 60Hz that are both present in the waveform I_a. The two centermost peaks are 120Hz (60Hz times 2) apart from 6kHz and there are sequential peak pairs an additional 120Hz further. For a proper Fourier analysis, the largest magnitude is

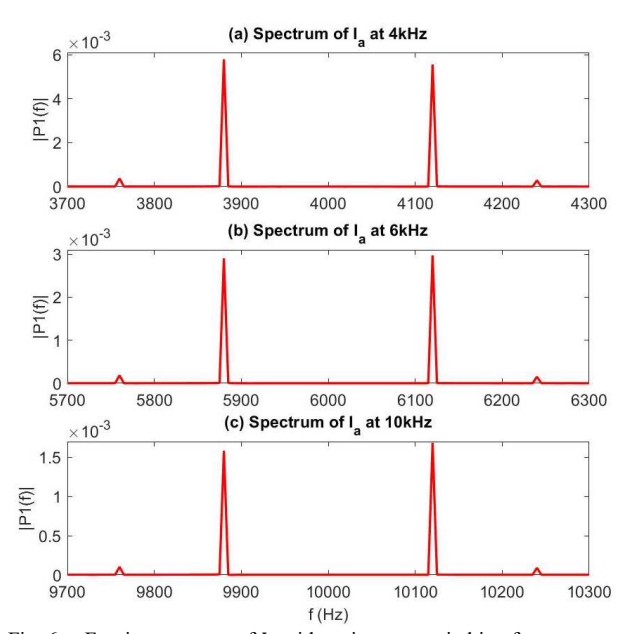


Fig. 6 Fourier spectrum of I_a with an inverter switching frequency of (a) 4kHz, (b) 6kHz, and (c) 10kHz.

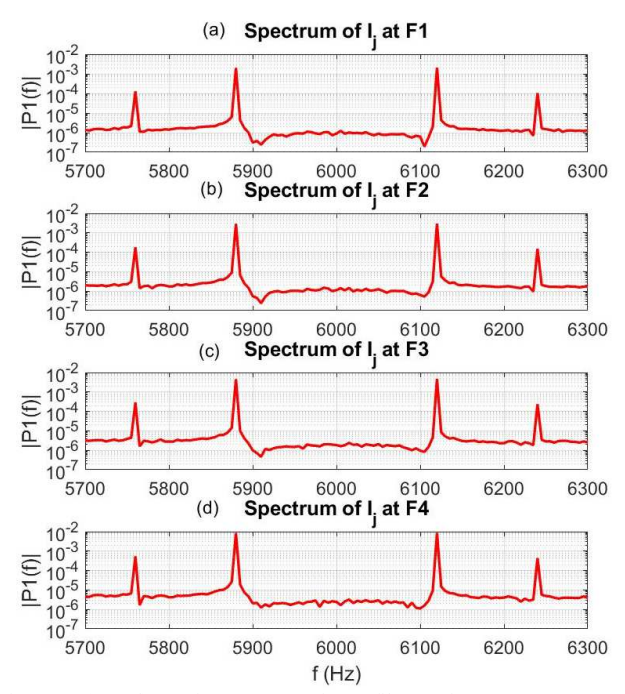


Fig. 7 (a) to (d) Fourier spectrum of I_a at filter settings F1 to F4, respectively, centered around 6kHz.

taken and compared with the magnitude of 60Hz. F1 producing an SNR (signal-to-noise ratio) of 27.58 and F4 producing 21.25 further asserts the superiority of the larger filter for GFMIs, at least as far as switch waves are concerned.

V. CONCLUSION

This design analyzed the impact the implementation of a grid-forming inverter would have on the traveling waves incident on the distribution lines, as opposed to a three-phase generator. When connecting a GFMI inverter to a distribution system one must be mindful of the effects it may have on the system, however these switching disturbances have small effects and can be addressed with proper filter design. Given that, proper design of power electronics can allow for efficient distribution of power across grids and other distribution systems due to the versatility of power electronics such as GFMIs. This is especially critical due to the implementation of relatively novel DC generation sources such as photovoltaic cells.

ACKNOWLEDGEMENT

This work was partially supported by the NSF Grants \#OIA-1757207 (NM EPSCoR), HRD-1345232, HRD-1914635 and funding from Sandia National Laboratories Campus Executive (CE) LDRD Supplemental Project 20-0656, and award number GR0006770 (SHAZAM), DOE NNSA MSIPP STEP2NLs; DOE Financial Assistance Award # DE-NA0003983 and funding from the Electric Utility Management Program (EUMP) at the New Mexico State University. Sandia National Laboratories is a multi-mission laboratory managed and operated by National Technology and Engineering Solutions of Sandia, LLC., a wholly owned subsidiary of Honeywell

International, Inc., for the U.S. Department of Energy's National Nuclear Security Administration under contract DE-NA0003525. The views expressed in the article do not necessarily represent the views of the U.S. Department of Energy or the United States Government.

REFERENCES

- Henderson, M.I., Novosel, D., & Crow, M.L. (2017). Electric Power Grid Modernization Trends, Challenges, and Opportunities.
- [2] M. Jiménez Aparicio, S. Grijalva, and M. J. Reno, "Fast Fault Location Method for a Distribution System with High Penetration of PV," Hawaii International Conference on System Sciences (HICSS), 2021.
- [3] S. Paul, S. Grijalva, M. Jiménez-Aparicio, and M. J. Reno, "Knowledge-based Fault Diagnosis for a Distribution System with High PV Penetration", IEEE Innovative Smart Grid Technologies (ISGT), 2022.
- [4] F. H. Magnago and A. Abur, "Fault location using wavelets," in IEEE Transactions on Power Delivery, vol. 13, no. 4, pp. 1475-1480, Oct. 1998, doi: 10.1109/61.714808.
- [5] Shilpa G, Sophi & Mokhlis, Hazlie & Illias, Hazlee. (2017). Fault location and detection techniques in power distribution systems with distributed generation: A review. Renewable and Sustainable Energy Reviews. 74. 949-958. 10.1016/j.rser.2017.03.021.
- [6] Ton, Dan & Smith, Merrill. (2012). The U.S. Department of Energy's Microgrid Initiative. The Electricity Journal. 25. 84–94. 10.1016/j.tej.2012.09.013.
- [7] J. Park and J. Candelaria, "Fault Detection and Isolation in Low-Voltage DC-Bus Microgrid System," in IEEE Transactions on Power Delivery,

- vol. 28, no. 2, pp. 779-787, April 2013, doi: 10.1109/TPWRD.2013.2243478.
- [8] D. Salomonsson, L. Soder and A. Sannino, "Protection of Low-Voltage DC Microgrids," in IEEE Transactions on Power Delivery, vol. 24, no. 3, pp. 1045-1053, July 2009, doi: 10.1109/TPWRD.2009.2016622.
- [9] E. Sortomme, S. S. Venkata and J. Mitra, "Microgrid Protection Using Communication-Assisted Digital Relays," in IEEE Transactions on Power Delivery, vol. 25, no. 4, pp. 2789-2796, Oct. 2010, doi: 10.1109/TPWRD.2009.2035810.
- [10] M. J. Reno, S. Brahma, A. Bidram, and M. E. Ropp, "Influence of Inverter-Based Resources on Microgrid Protection: Part 1: Microgrids in Radial Distribution Systems," IEEE Power and Energy Magazine, 2021.
- [11] F. Wilches-Bernal et al., "A Survey of Traveling Wave Protection Schemes in Electric Power Systems," in IEEE Access, vol. 9, pp. 72949-72969, 2021, doi: 10.1109/ACCESS.2021.3080234.
- [12] A. Reznik, M. G. Simões, A. Al-Durra and S. M. Muyeen, "\$LCL\$ Filter Design and Performance Analysis for Grid-Interconnected Systems," in IEEE Transactions on Industry Applications, vol. 50, no. 2, pp. 1225-1232, March-April 2014, doi: 10.1109/TIA.2013.2274612.
- [13] Dursun, Mustafa & Dosoglu, M.. (2018). LCL Filter Design for Grid Connected Three-Phase Inverter. 1-4. 10.1109/ISMSIT.2018.8567054.
- [14] Shah, Shahil. (2015). Step-by-step design of an LCL filter for three-phase grid interactive converter. 10.13140/RG.2.1.3883.6964.
- [15] On Smart City and Emerging Technology (ICSCET), 2018, pp. 1-4, doi: 10.1109/ICSCET.2018.8537391.
- [16] Ortiz, Leony, et al. "Hybrid AC/DC Microgrid Test System Simulation: Grid-Connected Mode." Heliyon, vol. 5, no. 12, Elsevier BV, Dec. 2019, p. e02862, doi:10.1016/j.heliyon.2019.e02862